nomenological coefficient which could be fitted with experiment. Assuming the most simple temperature dependence for this phenomenological coefficient, some qualitative conclusions were able to be drawn, which included a change in sign of the slope of the magnetic-dispersion–vs–temperature curve for temperatures slightly below T_N as one passed between so-called low- and high-frequency regions and the existence of a maximum in the magnetic-absorption-factor–vs–temperature above T_N for both the low- and high-frequency regions.

ACKNOWLEDGMENT

One of the authors (J. H. B.) wishes to express his gratitude to Professor P. W. Kasteleyn for the kind hospitality shown him during a sabbatical research year at the Lorentz Institute for Theoretical Physics, Leiden, The Netherlands, where parts of the final manuscript were prepared.

*Research sponsored by the Air Force Office of Scientific Research, Office of Aerospace Research, U. S. Air Force, under AFOSR Grant No. 68-1498.

[1]See, for example, the following review articles: M. E. Fisher, Rept. Progr. Phys. 30, 615 (1967); P. Heller, *ibid.* 30, 731 (1967). Also, in *Proceedings of the International School of Physics "Enrico Fermi" on Critical Phenomena, LI Course*, 1970 (Academic, New York, to be published).

[2]R. A. Ferrell, N. Menyhård, H. Schmidt, F. Schwabl, and P. Szépfalusy, Phys. Rev. Letters 18, 891 (1967); Phys. Letters 24A, 493 (1967); Ann. Phys. (N. Y.) 47, 565 (1968).

[3]B. I. Halperin and P. C. Hohenberg, Phys. Rev. Letters 19, 700 (1967); Phys. Rev. 177, 952 (1969).

[4]M. Fixman, Advan. Chem. Phys. 6, 175 (1964); J. Chem. Phys. 47, 2808 (1967).

[5]K. Kawasaki, Phys. Rev. 150, 291 (1966).

[6]L. P. Kadanoff and J. Swift, Phys. Rev. 166, 89 (1968); L. P. Kadanoff, J. Phys. Soc. Japan Suppl. 26, 122 (1969).

[7]See, for example, the following papers and references therein: M. Suzuki, Progr. Theoret. Phys. (Kyoto) 43, 882 (1970); B. U. Felderhof, Rept. Math. Phys. (to be published).

[8]T. Tanaka, P. H. E. Meijer, and J. H. Barry, J. Chem. Phys. 37, 1397 (1962); J. H. Barry, *ibid.* 45, 4172 (1966).

[9]Y. Takagi, Proc. Phys.-Math. Soc. Japan 23, 44 (1941); 23, 553 (1941); T. Muto and Y. Takagi, Solid State Phys. 1, 193 (1955).

[10]H. A. Bethe, Proc. Roy. Soc. (London) 150A, 552 (1935). For applications to Ising antiferromagnetism see V. Firgau, Ann. Physik (Leipzig) 40, 295 (1941); J. M. Ziman, Proc. Roy. Soc. (London) 64A, 1108 (1951); D. M. Burley, Physica 27, 768 (1961).

[11]P. W. Kasteleyn, Physica 22, 387 (1956).

[12]M. E. Fisher and M. F. Sykes, Physica 28, 919 (1962); 28, 939 (1962). For purposes of comparison one must, for notational agreement, change $J \to 2J$ in formulas of the present paper.

[13]S. R. de Groot and P. Mazur, *Non-Equilibrium Thermodynamics* (North-Holland, Amsterdam, 1961).

[14]R. Kikuchi, Ann. Phys. (N. Y.) 10, 127 (1960); Hughes Research Report No. 271, 1963 (unpublished).

[15]K. W. Mess, thesis (University of Leiden, The Netherlands, 1969) (unpublished).

PHYSICAL REVIEW B VOLUME 4, NUMBER 9 1 NOVEMBER 1971

Acoustical Faraday Effect in Antiferromagnetic Cr_2O_3†

M. Boiteux, P. Doussineau, B. Ferry, J. Joffrin, and A. Levelut
Laboratoire d'Ultrasons, Faculté des Sciences de Paris, Tour* 13, 9 *quai Saint-Bernard, Paris* 5e, *France*
(Received 8 March 1971)

The rotation of the plane of polarization of an ultrasonic wave in both the antiferromagnetic and flopped phases of the antiferromagnetic crystal Cr_2O_3 has been calculated and measured at 4.2 °K using 9-GHz sound waves. The Faraday effect is found to arise from a resonant interaction between phonons and low-frequency magnon modes, by single-ion magnetostriction. The values of magneto-elastic coupling constants G_{44} and G_{46} of Cr^{3+} in Cr_2O_3 are determined: $|G_{44}| \propto 4.5\ \mathrm{cm}^{-1}$, $|G_{46}| \simeq 2.5\ \mathrm{cm}^{-1}$.

I. INTRODUCTION

Rotation of the plane of polarization of an acoustical transverse wave in a magnetically polarized crystal has been recognized, for a long time, to be a tool for the study of magneto-elastic coupling in magnetic materials. Kittel[1] was the first to draw attention to the possibility of a Faraday effect in ferromagnetic crystals. The first experimental results have been reported on yttrium iron garnet crystals and the values of the transverse magnetostriction were deduced at different temperatures.[2,3]

Similar experiments were done on paramagnetic crystals[4] and in metals.[5] In this last case, differ-

ent characteristics of the orbits of the electrons were obtained.

The common feature of these experiments is the difference in the coupling between the two inverse circularly polarized ultrasonic waves with the orbital movement of the electrons. This coupling difference, introduced by the magnetic field, results in two new dispersion laws for the two circularly polarized waves whose degeneracy is removed. A rotation of the plane of polarization follows. It must be emphasized that this effect supposes that, before coupling occurs, the two circularly polarized waves are degenerate. For crystals, this property exists along acoustical axes (a name coined by analogy with the optical axes in electromagnetism). The six-, four-, and threefold axes are among the acoustical axes. In the last case, internal conical refraction is superimposed.

This paper is devoted to the study of the rotation of the plane of polarization of acoustical waves in antiferromagnetic crystals; it develops a short report published elsewhere.[6] The effect originates from the coupling between two circular phonon modes with a magnon mode. The coupling is particularly efficient when the two wave vectors and the two frequencies are nearly equal.

Experiments reported here have been made on Cr_2O_3 crystal, using 9-GHz ultrasonic waves propagating along the threefold axis (easy-magnetization axis) at helium temperature. The biasing magnetic field was parallel to this axis. The effect has been observed both in the antiferromagnetic phase and in the flopped phase.

In Sec. II of this paper some general properties of antiferromagnetic crystals are outlined, and in Secs. III and IV, a theoretical calculation of the rotatory power in both phases is presented. In Sec. V the experimental apparatus is described, and an interpretation of the different experimental results is given; the values of a few magnetoelastic coupling constants are obtained. As a conclusion, the results are summarized in Sec. VI, and some comments are made on the extension of these experiments to other materials.

II. GENERAL PROPERTIES OF ANTIFERROMAGNETIC CRYSTALS

A. Description of an Antiferromagnetic Crystal

There exist several types of antiferromagnets, the magnetic structures of which are more or less complex. Only simple antiferromagnets with two antiparallel sublattices with the nearest neighbors of a spin of one sublattice lying entirely on the other sublattice will be considered here. The magnetic excitations of the system are described in terms of noninteracting spin waves. This approximation is justified for Cr_2O_3 at 4.2 °K (temperature of experiment); moreover, the magnon lifetime at this temperature is much greater than the period of the ultrasonic wave.[7]

In magnetic crystals, the acoustical Faraday effect may be enhanced when the frequency and wave vector of a spin-wave mode can be made as close as possible to the frequency and wave vector of the propagating ultrasonic wave. In the antiferromagnetic phase, a magnetic field $\vec{H}$ applied parallel to the easy axis of magnetization removes the degeneracy of the spin waves, leading to high- and low-frequency magnon modes. One of the low-frequency modes can fulfill the previous condition, if its velocity is not greater than that of phonons. For a given value of the applied field $H = H_{sf}$ ($H_{sf} = 59$ kG in Cr_2O_3 at 4.2 °K),[8] the magnetization flops to a direction nearly perpendicular to the easy axis. The spin-wave theory shows that there exist in this flopped phase two spin-wave modes,[9] one of which has a relatively low and nearly constant frequency ("acoustic" mode), the other a frequency which is zero at the antiferromagnetic-flop transition, and which increases strongly when the magnetic field increases ("optical" mode); the coupling between the ultrasonic waves and the optical mode can lead to an observable acoustical Faraday effect.

B. Magnon-Phonon Interactions in Antiferromagnetic Crystals

Some aspects of phonon-magnon interactions in antiferromagnetic crystals have been discussed previously,[10,11] and experimental results on ultrasonic attenuation near the spin-flop transition have been partly explained by these interactions.[12–14] Use of 9-GHz waves, as has been previously reported,[15] allows us to discriminate between resonant magnon-phonon interaction and spin-flop transition, at least in the antiferromagnetic phase.

Different coupling mechanisms between elastic strains and magnetization of a crystal are possible. The Hamiltonian will be written in the different cases in terms of spin variables S_+ and S_-, and phonon strains or displacements. Only the strong-interaction terms, i.e., resonant type, between the phonons of fixed frequency ω and the antiferromagnetic spin-wave modes of the crystal will be taken into account.

1. *Volume Magnetostriction*

In antiferromagnetic compounds, the main contribution to the volume magnetostriction arises from the modulation of the exchange integral by the phonon field. This coupling mechanism has been previously studied[16]; it gives rise to the following coupling Hamiltonian:

$$\mathcal{H} = \sum_{\lambda q p} [A_{\lambda q p}(\alpha_\lambda \alpha^\dagger_{\lambda -q} a^\dagger_{qp} - \alpha^\dagger_\lambda \alpha_{\lambda -q} a_{qp}) + B_{\lambda q p}(\alpha_\lambda \beta_{\lambda -q} a^\dagger_{qp} - \alpha^\dagger_\lambda \beta^\dagger_{\lambda -q} a_{qp}) + A_{\lambda q p}(\beta_\lambda \beta^\dagger_{\lambda -q} a_{qp} - \beta^\dagger_\lambda \beta_{\lambda -q} a^\dagger_{qp})] , \quad (2.1)$$

where α and β are the usual operators describing the magnon modes and a the phonon modes.

This Hamiltonian gives a noticeable contribution to the thermal relaxation of magnons. However, for a fixed wave vector $\vec{q}$, the interaction energy is very weak, and the resulting phonon and magnon renormalization hardly modifies the dispersion curves. This coupling process will be neglected in the following.

Another contribution to volume magnetostriction is the modulation of magnetic dipole-dipole interaction[17]; this interaction mechanism can lead to resonant magnon-phonon processes. However, it can be easily shown that the coupling constants in this case are two orders of magnitude smaller than those resulting from single-ion magnetostriction.

2. *Single-Ion Magnetostriction*

The single-ion magnetostriction interaction assumes the form

$$\mathcal{H}' = \sum_{\alpha,\beta,\gamma,\delta} \sum_{i} G^{i}_{\alpha\beta,\gamma\delta} S_\alpha{}^i S_\beta{}^i \epsilon^i_{\gamma\delta} \,. \tag{2.2}$$

$G_{\alpha\beta,\gamma\delta}$ are the components of the magneto-elastic coupling tensor G; they are unchanged by permutation of α and β and γ and δ separately. The tensor is simplified by the geometrical symmetry of the site. Tables giving null components can be found in a paper by Dobrov.[18] More explicitly,

$$\begin{aligned}\mathcal{H}' = \sum_i \sum_{\gamma\delta} [&G^i_{yz,\gamma\delta}\{S_y{}^i, S_z{}^i\} + G^i_{xz,\gamma\delta}\{S_x{}^i, S_z{}^i\} \\ &+ G^i_{xy,\gamma\delta}\{S_x{}^i, S_y{}^i\} + G_{xx,\gamma\delta}(S_x{}^i)^2 \\ &+ G_{yy,\gamma\delta}(S_y{}^i)^2 + G^i_{zz,\gamma\delta}(S_z{}^i)^2]\epsilon^i_{\gamma\delta} \,, \end{aligned} \tag{2.3}$$

where $\{S_\alpha, S_\beta\} = S_\alpha S_\beta + S_\beta S_\alpha$.

The spins point along the z axis, which is taken as quantization axis. Then three kinds of terms can be obtained.

Zero-order terms in spin variables S_+ or S_-. They come from $S_z{}^2$. They do not couple phonons and magnons because they cannot induce transitions between different magnon states.

Quadratic terms in spin variables. They come from the expressions of $S_x{}^2$, $S_y{}^2$, and $\{S_x, S_y\}$ as function of S_+ and S_-. The resulting coupling process is of the same type as that of volume magnetostriction (three-particle collisions). They will also be neglected.

Linear terms in spin variables. The expressions of $\{S_x, S_z\}\epsilon$ and $\{S_y, S_z\}\epsilon$ in terms of S_+ and S_- give a sum of terms linear in spin operators and linear in strains. They give rise to a possible resonant coupling, resulting from the following elementary process:

$$\text{phonon } (\omega, \vec{q}) \rightarrow \text{magnon } (\omega, \vec{q}) \text{ (and inverse process)} \,.$$

The contribution of this process to the thermal relaxation of magnons is negligible, because it occurs only in the vicinity of the crossing point where the phonon and magnon dispersion curves intersect. However, if a phonon mode or a magnon mode of frequency and wave vector close to this crossing point is strongly excited, the coupling energy can be large. The propagating waves are then mixed waves, carrying elastic and magnetic energy; their dispersion law is different from those of pure phonons or pure magnons. They are called magneto-elastic waves. For the study of the acoustical effect, the system satisfies this condition. Furthermore, it will be pointed out that the modification of the phonon dispersion curves resulting from this resonant process is sensitive even rather far from the crossing point.

3. *Single-Ion Magnetostriction in* Cr_2O_3

In Cr_2O_3, the crystallographic sites of the magnetic ions Cr^{3+} have a C_3 symmetry. There are two types of sites; one is obtained from the other by a rotation of π around a twofold axis of the crystal. These two types of sites correspond to the two magnetic sublattices l and m.

For transverse waves propagating along the threefold axis (z axis), only strains ϵ_{xz} and ϵ_{yz} are different from zero. Therefore, the coupling constants of interest are G_{41}, G_{44}, G_{45}, and G_{46}. Between the constants relative to sites l and m exist the relations

$$G^l_{41} = G^m_{41}, \quad G^l_{44} = G^m_{44}, \quad G^l_{45} = -G^m_{45}, \quad G^l_{46} = -G^m_{46} \,. \tag{2.4}$$

Axes x and y, which are not imposed by the C_3 symmetry, have been chosen identical to those of the crystal (imposed by the D_{3d} symmetry).

The interaction Hamiltonian is therefore written

$$\begin{aligned}\mathcal{H}' = \sum_l \{&(G_{41}[(S_x{}^l)^2 - (S_y{}^l)^2] + G_{44}\{S_y{}^l, S_z{}^l\} + G_{45}\{S_x{}^l, S_z{}^l\} + G_{46}\{S_x{}^l, S_y{}^l\})e^l_{yz} \\ &+ (-G_{46}[(S_x{}^l)^2 - (S_y{}^l)^2] - G_{45}\{S_y{}^l, S_z{}^l\} + G_{44}\{S_x{}^l, S_z{}^l\} + G_{41}\{S_x{}^l, S_y{}^l\})e^l_{xz}\} \\ &+ \sum_m \{(G_{41}[(S_x{}^m)^2 - (S_y{}^m)^2] + G_{44}\{S_y{}^m, S_z{}^m\} - G_{45}\{S_x{}^m, S_z{}^m\} - G_{46}\{S_x{}^m, S_y{}^m\})e^m_{yz} \\ &+ (G_{46}[(S_x{}^m)^2 - (S_y{}^m)^2] + G_{45}\{S_y{}^m, S_z{}^m\} + G_{44}\{S_x{}^m, S_z{}^m\} + G_{41}\{S_x{}^m, S_y{}^m\})e^m_{xz}\} \,, \end{aligned} \tag{2.5}$$

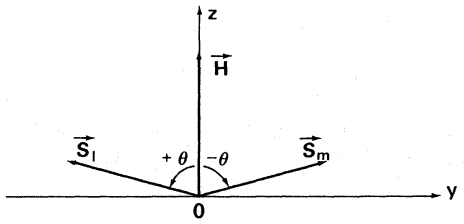

FIG. 1. Spin configuration of each sublattice in the flopped phase.

where e_{xz} and e_{yz} are related to tensorial strains by

$$2\epsilon_{xz}=e_{xz}, \quad 2\epsilon_{yz}=e_{yz}.$$

In the antiferromagnetic phase, the spins of each sublattice point along the z axis. The terms which give a noticeable contribution are those coming from $\{S_x^i, S_z^i\}$ and $\{S_y^i, S_z^i\}$.

In the flopped phase, the sublattice l is rotated by an angle θ about the x axis and the sublattice m by an angle $-\theta$ (Fig. 1). New spin components $\tilde{S}_\alpha{}^i$ can be defined such as

$$\begin{aligned} &S_x^l=\tilde{S}_x^l, && S_x^m=\tilde{S}_x^m,\\ &S_y^l=\cos\theta\tilde{S}_y^l-\sin\theta\tilde{S}_z^l, && S_y^m=\cos\theta\tilde{S}_y^m+\sin\theta\tilde{S}_z^m,\\ &S_z^l=\sin\theta\tilde{S}_z^l+\cos\theta S_z^l, && S_z^m=-\sin\theta\tilde{S}_y^m+\cos\theta\tilde{S}_z^m. \end{aligned} \tag{2.6}$$

The main contribution to $\mathcal{H}'$ arises from the terms of the type $\{\tilde{S}_z^i, \tilde{S}_x^i\}$ and $\{\tilde{S}_y^i, \tilde{S}_z^i\}$.

These results are now used to calculate the rotation of the plane of polarization in the two phases.

III. ANTIFERROMAGNETIC PHASE

A. Phonon Hamiltonian

For a phonon mode of wave vector $\vec{q}$ and polarization i, the Hamiltonian is

$$\mathcal{H}_{q,i}=\hbar\omega_{qi}(a_{qi}^\dagger a_{qi}+\tfrac{1}{2}). \tag{3.1}$$

In the problem treated here, two linear polarizations occur, $i=x, y$. But, as was pointed out in the Introduction, circularly polarized vibrations play an essential part. If the calculation were conducted by a perturbation method, these polarizations would be imposed because they have the symmetry of the perturbed system. However, in the present work, since an exact diagonalization is performed, a change of reference modes may be achieved indifferently at the beginning (choice of linear or circular vibrations) or at the end of the calculation (final diagonalization). Usually the spin-phonon interaction Hamiltonians are given using linear phonon operators (i.e., with ϵ_{xy} and ϵ_{yz}); therefore linear vibrations have been used.

Because the spin-flop transition is not accompanied by a structural phase transition, this phonon Hamiltonian describes with the same constants the ultrasonic wave in the antiferromagnetic phase as well as in the flopped phase.

B. Antiferromagnetic Magnon Hamiltonian

The Hamiltonian

$$\mathcal{H}_m=J\sum_{j,\delta}\vec{S}_j\cdot\vec{S}_{j+\delta}-2\mu_B H_A\sum_l S_z^l+2\mu_B H_A\sum_m S_z^m \tag{3.2}$$

has to be transformed in magnon variables. This is usually achieved by Holstein-Primakoff, then Bogoliubov transformations.[19] Here, this is done within the usual low-temperature approximation.

So, new variables are successively introduced by

$$\begin{aligned} &S_z^l=S, && S_z^m=-S,\\ &S_+^l=(2S)^{1/2}c_l, && S_+^m=(2S)^{1/2}d_m^\dagger,\\ &S_-^l=(2S)^{1/2}c_l^\dagger, && S_-^m=(2S)^{1/2}d_m, \end{aligned} \tag{3.3}$$

where

$$\begin{aligned} &c_l=(N)^{-1/2}\textstyle\sum_{k'} e^{-i\vec{k}'\cdot\vec{R}_l}c_{k'},\\ &d_m=(N)^{-1/2}\textstyle\sum_{k''} e^{i\vec{k}''\cdot\vec{R}_m}d_{k''}. \end{aligned} \tag{3.4}$$

Finally, the magnon operators α_k, β_k are given by

$$\begin{aligned} &c_k=\alpha_k\cosh\theta_k+\beta_k^\dagger\sinh\theta_k,\\ &d_k=\alpha_k^\dagger\sinh\theta_k+\beta_k\cosh\theta_k, \end{aligned} \tag{3.5}$$

with

$$\gamma_k=(1/z)\textstyle\sum_\delta e^{i\vec{k}\cdot\vec{\delta}}, \tag{3.6}$$

where z is the number of nearest neighbors.

The magnon Hamiltonian is then

$$\mathcal{H}_m=\textstyle\sum_k\hbar\,\Omega_k(\alpha_k^\dagger\alpha_k+\frac{1}{2})+\hbar\,\Omega_k(\beta_k^\dagger\beta_k+\frac{1}{2}); \tag{3.7}$$

with $\Omega_k>0$,

$$\Omega_k^2=(\omega_E+\omega_A)^2-\omega_E^2\gamma_k^2. \tag{3.8}$$

In the domain of interest, $a^2k^2\ll1$ and

$$\gamma_k^2\simeq 1-\lambda a^2k^2. \tag{3.9}$$

This scheme perhaps oversimplifies the situation of antiferromagnetic Cr_2O_3,[20] but it is correct in the limit of small wave vectors ($ka\ll H_A/H_E$). If a magnetic field is applied parallel to the easy-magnetization axis, the degeneracy of magnons α_k and β_k is removed:

$$\Omega_\alpha(k,H)=\Omega_k+\gamma H, \quad \Omega_\beta(k,H)=\Omega_k-\gamma H, \quad \gamma=g\mu_B/\hbar. \tag{3.10}$$

C. Interaction Hamiltonian

Starting with the Hamiltonian

$$\mathcal{H}'=\textstyle\sum_l\{(G_{44}\{S_y^l, S_z^l\}+G_{45}\{S_x^l, S_z^l\})e_{yz}^l + (-G_{45}\{S_y^l, S_z^l\}+G_{44}\{S_x^l, S_z^l\})e_{xz}^l\}$$

$$+\sum_m\{(G_{44}\{S_y^m, S_z^m\}-G_{45}\{S_x^m, S_z^m\})e_{yz}^m$$

$$+(G_{45}\{S_y^m, S_z^m\}+G_{44}\{S_x^m, S_z^m\})e_{xz}^m\}\ , \quad (3.11)$$

using the preceding transformations (3.2)–(3.4) and the development of $e(\vec{q})$ as a function of the phonon operators, it is found that magnons of wave vector $\vec{q}$ are coupled to phonons of wave vectors $+\vec{q}$ and $-\vec{q}$. Therefore every operator a_q must be accompanied by a_{-q}.

Then, for the mode j,

$$e_{zj}=(\hbar\omega/2NMv_{us}^2)^{1/2}\, i[(a_{qj}+a_{-qj}^\dagger)\, e^{i\vec{q}\cdot\vec{R}} - (a_{qj}^\dagger+a_{-qj})\, e^{-i\vec{q}\cdot\vec{R}}], \quad (3.12)$$

where the time dependence has not been specified. N is the number of Cr^{3+} ions in each sublattice, NM is the total mass of the crystal, and v_{us} is the phonon or ultrasonic phase velocity.

Introducing coupling constants

$$A_1=S(2S)^{1/2}(\hbar\omega/2Mv_{us}^2)^{1/2}G_{44}(\sinh\theta_q-\cosh\theta_q)\ , \quad (3.13)$$

$$A_2=S(2S)^{1/2}(\hbar\omega/2Mv_{us}^2)^{1/2}G_{45}(\sinh\theta_q+\cosh\theta_q)\ ,$$

a new form of the interaction Hamiltonian is obtained:

$$\begin{aligned}\mathcal{H}' = {} & (A_1+iA_2)[\beta_q^\dagger(a_{qy}+a_{-qy}^\dagger)-\beta_{-q}^\dagger(a_{qy}^\dagger+a_{-qy})]+(A_1-iA_2)[\beta_q(a_{qy}^\dagger+a_{-qy})-\beta_{-q}(a_{qy}+a_{-qy}^\dagger)]\\ & -(A_2-iA_1)[\beta_q^\dagger(a_{qx}+a_{-qx}^\dagger)-\beta_{-q}^\dagger(a_{qx}^\dagger+a_{-qx})]-(A_2+iA_1)[\beta_q(a_{qx}^\dagger+a_{-qx})-\beta_{-q}(a_{qx}+a_{-qx}^\dagger)]\\ & -(A_1-iA_2)[\alpha_q(a_{qy}+a_{-qy}^\dagger)-\alpha_{-q}(a_{qy}^\dagger+a_{-qy})]-(A_1+iA_2)[\alpha_q^\dagger(a_{qy}^\dagger+a_{-qy})-\alpha_{-q}^\dagger(a_{qy}+a_{-qy}^\dagger)]\\ & -(A_2+iA_1)[\alpha_q(a_{qx}+a_{-qx}^\dagger)-\alpha_{-q}(a_{qx}^\dagger+a_{-qx})]-(A_2-iA_1)[\alpha_q^\dagger(a_{qx}^\dagger+a_{-qx})-\alpha_{-q}^\dagger(a_{qx}+a_{-qx}^\dagger)]\ . \quad (3.14)\end{aligned}$$

The total Hamiltonian is

$$\mathcal{H}=\mathcal{H}_m+\mathcal{H}_p+\mathcal{H}'\ ,$$

where

$$\mathcal{H}_m=\hbar\Omega_\alpha(q)[(\alpha_q^\dagger\alpha_q+\tfrac{1}{2})+(\alpha_{-q}^\dagger\alpha_{-q}+\tfrac{1}{2})]+\hbar\Omega_\beta(q)[(\beta_q^\dagger\beta_q+\tfrac{1}{2})+(\beta_{-q}^\dagger\beta_{-q}+\tfrac{1}{2})], \quad (3.15a)$$

$$\mathcal{H}_p=\hbar\omega(q)[(a_{qx}^\dagger a_{qx}+\tfrac{1}{2})+(a_{-qx}^\dagger a_{-qx}+\tfrac{1}{2})+(a_{qy}^\dagger a_{qy}+\tfrac{1}{2})+(a_{-qy}^\dagger a_{-qy}+\tfrac{1}{2})]\ . \quad (3.15b)$$

D. Dispersion Law of Magneto-Elastic Waves

The problem is now to determine the eigenfrequencies of vibration of the system. Each operator α, β, and a satisfies the boson commutation rule $[Q, Q^\dagger]=1$ and follows the evolution equation $i\hbar\, dQ/dt=[Q,\mathcal{H}]$, which can be written

$$\begin{aligned}
i\hbar\, da_{qy}/dt &= \hbar\omega a_{qy}+(A_1-iA_2)\,\alpha_{-q}-(A_1+iA_2)\,\alpha_q^\dagger+(A_1-iA_2)\beta_q-(A_1+iA_2)\beta_{-q}^\dagger\ ,\\
i\hbar\, da_{-qy}^\dagger/dt &= -\hbar\omega a_{-qy}^\dagger-(A_1-iA_2)\alpha_{-q}+(A_1+iA_2)\alpha_q^\dagger-(A_1-iA_2)\beta_q+(A_1+iA_2)\beta_{-q}^\dagger\ ,\\
i\hbar\, da_{qx}/dt &= \hbar\omega a_{qx}+(A_2+iA_1)\alpha_{-q}-(A_2-iA_1)\alpha_q^\dagger-(A_2+iA_1)\beta_q+(A_2-iA_1)\beta_{-q}^\dagger\ ,\\
i\hbar\, da_{-qx}^\dagger/dt &= -\hbar\omega a_{-qx}^\dagger-(A_2+iA_1)\alpha_{-q}+(A_2-iA_1)\alpha_q^\dagger+(A_2+iA_1)\beta_q-(A_2-iA_1)\beta_{-q}^\dagger\ ,\\
i\hbar\, d\alpha_{-q}/dt &= \hbar\Omega_\alpha\,\alpha_{-q}+(A_1+iA_2)(a_{qy}+a_{-qy}^\dagger)+(A_2-iA_1)(a_{qx}+a_{-qx}^\dagger)\ ,\\
i\hbar\, d\alpha_q^\dagger/dt &= -\hbar\Omega_\alpha\,\alpha_q^\dagger+(A_1-iA_2)(a_{qy}+a_{-qy}^\dagger)+(A_2+iA_1)(a_{qx}+a_{-qx}^\dagger)\ ,\\
i\hbar\, d\beta_q/dt &= \hbar\Omega_\beta\beta_q+(A_1+iA_2)(a_{qy}+a_{-qy}^\dagger)-(A_2-iA_1)(a_{qx}+a_{-qx}^\dagger)\ ,\\
i\hbar\, d\beta_{-q}^\dagger/dt &= -\hbar\Omega_\beta\beta_{-q}^\dagger+(A_1-iA_2)(a_{qy}+a_{-qy}^\dagger)-(A_2+iA_1)(a_{qx}+a_{-qx}^\dagger)\ .
\end{aligned} \quad (3.16)$$

Now, using variables describing circularly polarized phonons

$$a_{qx}\pm ia_{qy}=a_{q\pm}\ ,\quad a_{-qx}^\dagger\pm ia_{-qy}^\dagger=a_{-q\pm}^\dagger\ ,$$

the set of equations (3.16) can be written

$$i\hbar\, d\vec{X}/dt=A\vec{X}\ , \quad (3.17)$$

with $\vec{X}=(a_{q+}, a_{q-}, a_{-q+}^\dagger, a_{-q-}^\dagger, \alpha_{-q}, \alpha_q^\dagger, \beta_q, \beta_{-q}^\dagger)$ and

$$A = \begin{vmatrix} \hbar\omega & & & & 2(A_2+iA_1) & & & 2(A_2-iA_1) \\ & \hbar\omega & & & & -2(A_2-iA_1) & -2(A_2+iA_1) & \\ & & -\hbar\omega & & -2(A_2+iA_1) & & & -2(A_2-iA_1) \\ & & & -\hbar\omega & & 2(A_2-iA_1) & 2(A_2+iA_1) & \\ A_2-iA_1 & & A_2-iA_1 & & \hbar\Omega_\alpha & & & \\ & A_2+iA_1 & & A_2+iA_1 & & -\hbar\Omega_\alpha & & \\ & -(A_2-iA_1) & & -(A_2-iA_1) & & & \hbar\Omega_\beta & \\ -(A_2+iA_1) & & -(A_2+iA_1) & & & & & -\hbar\Omega_\beta \end{vmatrix} \tag{3.18}$$

The equations relative to the eight other operators lead to the same solutions.

The eigenfrequencies ω_{me} of the magneto-elastic waves and the eigenfunctions can be determined by diagonalization of the matrix A appearing in (3.17), which is the direct sum of two 4×4 matrices. Each of these operates in a vectorial space spanned by variables a_{q+}, a^+_{-q+}, α_{-q}, and β^+_{-q}, and by a_{q-}, a_{-q-}, α^+_q, and β_q, respectively.

These two matrices lead to the two following dispersion laws:

$$(\omega_{me}^2-\omega^2)[(\omega_{me}+\omega_0)^2-\omega_c^2]-8\omega\omega_c\frac{A_1^2+A_2^2}{\hbar^2}=0\ , \tag{3.19}$$

$$(\omega_{me}^2-\omega^2)[(\omega_{me}-\omega_0)^2-\omega_c^2]-8\omega\omega_c\frac{A_1^2+A_2^2}{\hbar^2}=0\ , \tag{3.20}$$

where

$$2\omega_c=\Omega_\alpha+\Omega_\beta\ ,\quad 2\omega_0=\Omega_\alpha-\Omega_\beta\ .$$

If $\vec{H}=0$ ($\omega_0=0$), the two equations are identical and lead to identical roots. The two magneto-elastic modes are always excited in pairs [Fig. 2(a)] with equal phase velocities; therefore no rotation of the plane of polarization can occur. If $\vec{H}\neq0$, the degeneracy of the magneto-elastic modes is removed, as can be seen in Fig. 2(b). In Cr_2O_3, $H_E=2.4\times10^6$ G and $H_A=700$ G. Then $\tanh2\theta_q\simeq-1$ and $\cosh\theta_q\simeq-\sinh\theta_q$. Therefore, if G_{45} is not much greater than G_{44},

$$\frac{A_2}{A_1}=\frac{\cosh\theta_q+\sinh\theta_q}{\cosh\theta_q-\sinh\theta_q}\frac{G_{45}}{G_{44}}\ll1\ .$$

Under these conditions A_2 can be neglected. The two positive roots arising from the dispersion equations and whose values are nearly equal to $v_{us}q$ are

$$\omega_{me0}=\omega+4\omega_c(A_1^2/\hbar^2)[(\omega-\omega_0)^2-\omega_c^2]^{-1}\ ,\quad \text{mode 0} \tag{3.21a}$$

$$\omega_{me1}=\omega+4\omega_c(A_1^2/\hbar^2)[(\omega+\omega_0)^2-\omega_c^2]^{-1}\ ,\quad \text{mode 1}\ . \tag{3.21b}$$

The third magneto-elastic mode of relatively low frequency ($\omega_{me}\simeq\Omega_\beta$) has a dispersion law

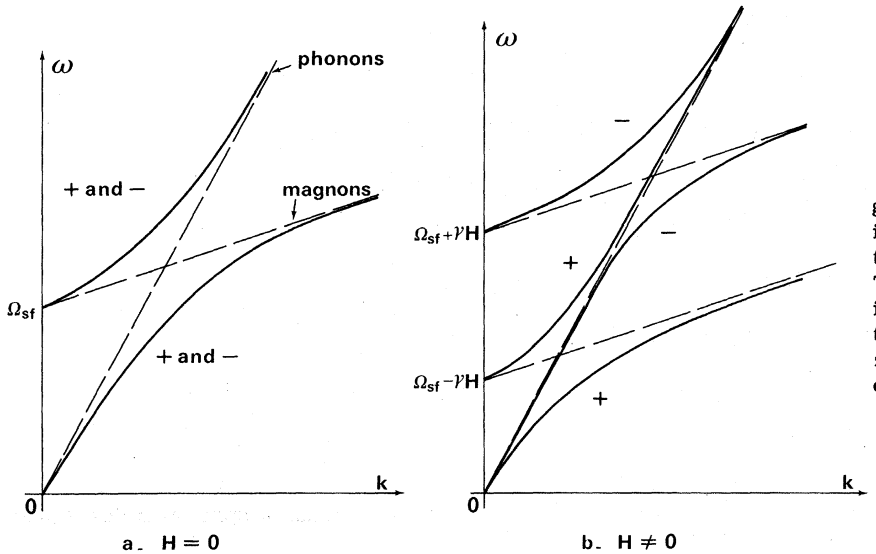

FIG. 2. Removal of the degeneracy of magneto-elastic waves in the antiferromagnetic phase by the application of a magnetic field. The dashed curves relate to non-interacting magnons and phonons, the full curves with relative polarizations + and − relate to magneto-elastic modes.

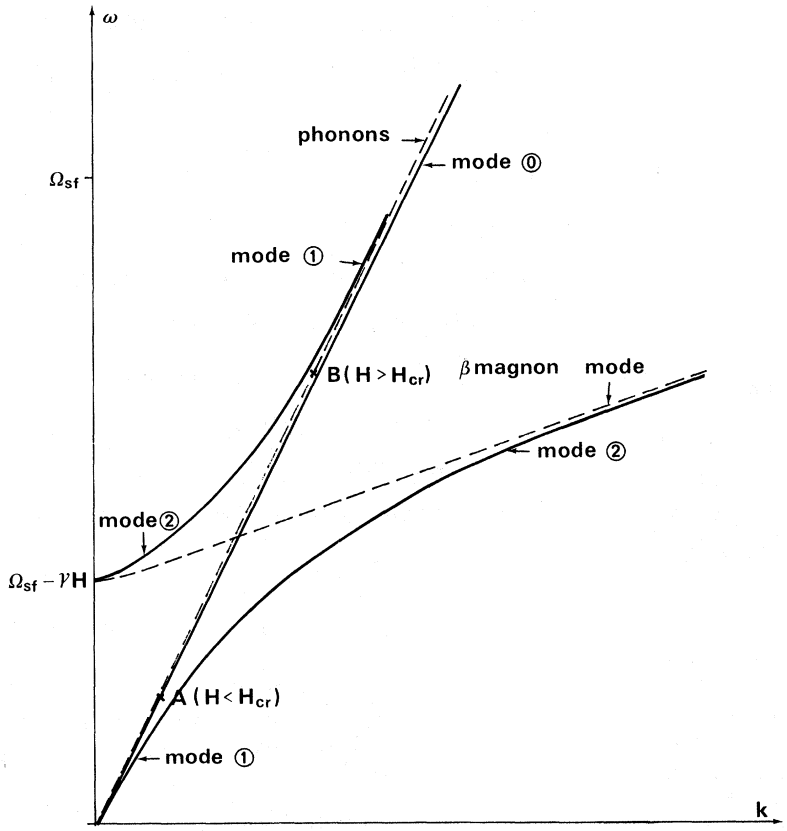

FIG. 3. Dispersion curves of magneto-elastic modes 0, 1, and 2 in the antiferromagnetic phase [see Eqs. (3.22a)–(3.22c)]. The field H_{cr} is defined by $\Omega_\beta(q, H=H_{cr}) = \omega(q)$. Both the magneto-elastic modes 0 and 1 are preferentially excited: near A when $H<H_{cr}$ and near B when $H>H_{cr}$.

$$\omega_{me} = \Omega_\beta + (4\omega A_1^2/\hbar^2)[(\omega_c - \omega_0)^2 - \omega^2]^{-1}, \text{ mode 2.} \tag{3.22}$$

These formulas are valid provided that the following conditions hold:

$$\hbar^2(\Omega_\beta^2 - \omega^2)^2 \gg 8\omega\Omega_\beta A_1^2 , \tag{3.23a}$$

$$\hbar^2(\Omega_\beta^2 - \omega^2) \gg \Omega_\beta A_1^2 , \tag{3.23b}$$

$$\hbar^2\omega\Omega_\beta \gg 2A_1^2 . \tag{3.23c}$$

In Fig. 3 the dispersion curves of the three magneto-elastic modes are plotted. H_{cr} is the value of H for which $\omega(q) = \Omega_\beta(q)$. If H is not very close to H_{cr}, there are always two magneto-elastic modes which are preferentially excited (modes 0 and 1); they are circularly polarized in opposite senses and they have different phase velocities. The resultant linear polarization, arising from one round trip through the crystal, depends on the phase difference between the two waves, i.e., on magnetic field. It must be noticed that the frequencies which have been calculated correspond to a given wave vector. In fact, experiments are made at a given frequency. Nevertheless, the preceding results are quite correct if the phase velocities are not too strongly modified.

E. Faraday Rotation

The rotation per unit length can be written

$$\xi/l = \tfrac{1}{2}(k_1 - k_0) = \tfrac{1}{2}\omega\Delta v/v_{us}^2 = A\,\Omega/(\Omega^2 - \omega^2) ,$$

with

$$A = (2S^3\omega/Mv_{us}^3\hbar)G_{44}^2(\sinh\theta_q - \cosh\theta_q)^2 ,$$

$$\tanh 2\theta_q = -H_E\gamma_q/(H_E + H_A) ,$$

$$|\tanh 2\theta_q| \gg 1 ,$$

from which

$$\cosh\theta_q \neq -\sinh\theta_q \neq \tfrac{1}{2}e^{-\theta_q} = \frac{1}{2}\left(\frac{2}{\lambda(qa)^2 + H_A/H_E}\right)^{1/4} ,$$

where λ is given by $\gamma_q \sim 1 - \lambda(qa)^2$. Thus,

$$\frac{\xi}{l} = \frac{2S^3 G_{44}^2}{Mv_{us}^3\hbar}\left(\frac{2}{\lambda(qa)^2 + H_A/H_E}\right)^{1/2}\frac{\omega^2}{\Omega^2 - \omega^2} . \tag{3.24}$$

IV. FLOPPED PHASE

A. Magnon Hamiltonian

The magnon spectrum in the flopped phase of an antiferromagnet can be determined in a way similar to that of the antiferromagnetic phase.[9] The Hamiltonian (3.2) remains unchanged and the diagonalization is achieved by the following steps.

(i) Quantization of each sublattice in axes rotated by $+\theta$ and $-\theta$ around the x axis [Eqs. (2.6)].

(ii) Fourier transforms of spin variables $\tilde{S}_+$ and $\tilde{S}_-$:

$$\tilde{S}_x^{\,l} = S\ ,\quad \tilde{S}_x^{\,m} = S\ ,$$

$$\tilde{S}_+^{\,l} = \left(\frac{2S}{N}\right)^{1/2} \sum_{k'} e^{-i\vec{k}'\cdot\vec{R}_l}\, c_{k'}\ ,$$

$$\tilde{S}_+^{\,m} = \left(\frac{2S}{N}\right)^{1/2} \sum_{k'} e^{-i\vec{k}'\cdot\vec{R}_m}\, d_{k'}\ , \qquad (4.1)$$

$$\tilde{S}_-^{\,l} = \left(\frac{2S}{N}\right)^{1/2} \sum_{k'} e^{i\vec{k}'\cdot\vec{R}_l}\, c_{k'}^{\dagger}\ ,$$

$$\tilde{S}_-^{\,m} = \left(\frac{2S}{N}\right)^{1/2} \sum_{k'} e^{i\vec{k}'\cdot\vec{R}_m}\, d_{k'}^{\dagger}\ .$$

(iii) Holstein-Primakoff-type transformation:

$$c_k = A_k\,\alpha_k + B_k\,\alpha_{-k}^{\dagger} + C_k\,\beta_{-k} + D_k\,\beta_k^{\dagger}\ , \qquad (4.2a)$$

$$d_k = -A_k\,\alpha_k - B_k\,\alpha_{-k}^{\dagger} + C_k\,\beta_{-k} + D_k\,\beta_k^{\dagger}\ . \qquad (4.2b)$$

The ultrasonic waves interact with the "optical" mode (β mode) of wave vector $\vec{q}$. The frequency of this mode is

$$\Omega(q) = (g\mu_B/\hbar)\,[H_E(1+\gamma_k)]^{1/2} \times [H_E(1+\gamma_k\cos 2\theta) - H_A\sin^2\theta]^{1/2}\ , \qquad (4.3)$$

$\Omega(q)$ depending on the magnetic field $\vec{H}$ through θ.

The ultrasonic waves can also interact with the low-frequency magnon mode, leading to a rotation of the plane of polarization. However, the frequency of this mode is nearly independent of the magnetic field such that variations of the rotation angle as function of H cannot be observed experimentally.

B. Interaction Hamiltonian

In the interaction Hamiltonian (2.5), only the terms linear in $\tilde{S}_+$ or $\tilde{S}_-$ and linear in ϵ are retained. This Hamiltonian can be written using the transformations (4.1) and (4.2):

$$\mathcal{H} = G_1 A_-[(\beta_q - \beta_{-q}^{\dagger})(a_{qy} + a_{-qy}^{\dagger}) + (\beta_q^{\dagger} - \beta_{-q})(a_{qy}^{\dagger} + a_{-qy})]$$
$$- iG_2 A_+[(\beta_q + \beta_{-q}^{\dagger})(a_{qy} + a_{-qy}^{\dagger}) - (\beta_q^{\dagger} + \beta_{-q})(a_{qy}^{\dagger} + a_{-qy})]$$
$$- G_3 A_-[(\beta_q - \beta_{-q}^{\dagger})(a_{qx} + a_{-qx}^{\dagger}) + (\beta_q^{\dagger} - \beta_{-q})(a_{qx}^{\dagger} + a_{-qx})]$$
$$+ iG_4 A_+[(\beta_q + \beta_{-q}^{\dagger})(a_{qx} + a_{-qx}^{\dagger}) - (\beta_q^{\dagger} + \beta_{-q})(a_{qx}^{\dagger} + a_{-qx})]\ , \qquad (4.4)$$

where

$$A_+ = C_q + D_q\ ,$$

$$A_- = C_q - D_q\ ,$$

$$G_1 = S(2S)^{1/2}(\hbar\omega/2Mv_{us}^2)^{1/2}\,G_{44}(\cos^2\theta - \sin^2\theta)\ ,$$

$$G_2 = S(2S)^{1/2}(\hbar\omega/2Mv_{us}^2)^{1/2}\,G_{46}\sin\theta\ ,$$

$$G_3 = S(2S)^{1/2}(\hbar\omega/2Mv_{us}^2)^{1/2}\,G_{46}\sin\theta\cos\theta\ ,$$

$$G_4 = S(2S)^{1/2}(\hbar\omega/2Mv_{us}^2)^{1/2}\,G_{44}\cos\theta\ .$$

C. Dispersion Relation for Magneto-Elastic Waves

The equations of motion lead to the dispersion relation

$$(\omega^2 - \omega_{me}^2)\{\hbar^4(\omega^2 - \omega_{me}^2)(\Omega^2 - \omega_{me}^2) - 4\hbar^2\omega\Omega[(G_1A_-)^2 + (G_2A_-)^2 + (G_3A_-)^2 + (G_4A_+)^2]\} + 16(G_1G_4 - G_2G_3)^2(A_+A_-)^2\omega^2 = 0\ . \qquad (4.5)$$

In the same approximation that was used for the antiferromagnetic phase, three magneto-elastic modes are obtained.

D. Faraday Rotation

The rotation of the plane of polarization per unit length is given by

$$\frac{\xi}{l} = \frac{S^3G^2}{Mv_{us}^3\hbar}\,\frac{\omega\Omega}{\Omega^2 - \omega^2}\ , \qquad (4.6)$$

where

$$G^2 = G_{44}^2[A(\cos^2\theta - \sin^2\theta)^2 + (\cos^2\theta)/A] + G_{46}[\sin^2\theta\,(A\cos^2\theta + 1/A)]. \qquad (4.7)$$

In the following, the values of Ω and A will be taken at $k = 0$. In the long-wavelength limit,

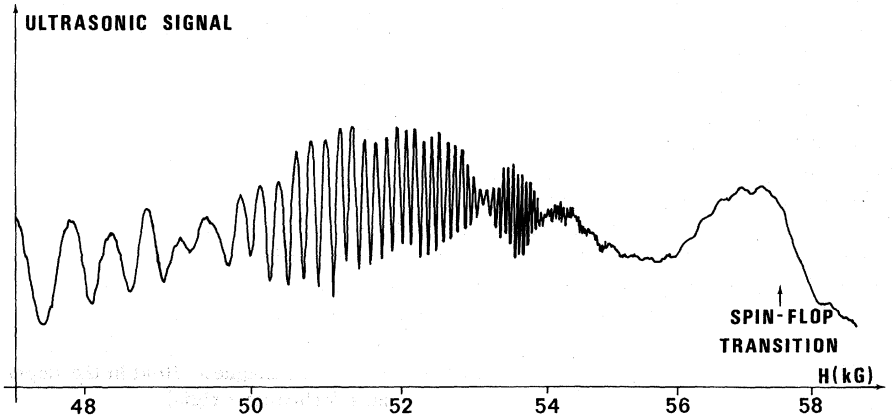

FIG. 4. Ultrasonic signal as a function of magnetic field in the antiferromagnetic phase of Cr_2O_3 at 4.2 °K and 8890 MHz. The crystal is 4.4 mm long. The magnetic field is applied parallel to the c axis of the crystal with an accuracy better than 0.5°. Each oscillation of the signal corresponds to a rotation of π of the ultrasonic polarization.

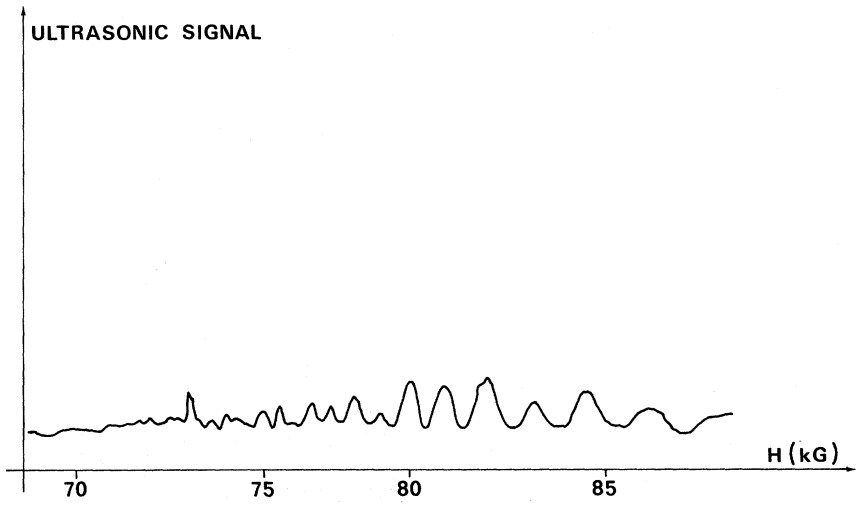

FIG. 5. Ultrasonic signal as a function of magnetic field in the flopped phase of Cr_2O_3, in the same conditions as those of Fig. 4.

$qa \ll 1$, and $\Omega(k)$ and $A(k)$ take the following values for $k \to 0$:

$$\hbar\Omega = g\mu_B (4H_E^2 \cos^2\theta - 2H_E H_A \sin^2\theta)^{1/2} , \tag{4.8}$$

$$A = 4\left(\frac{2H_E}{2H_E \cos^2\theta - H_A \sin^2\theta}\right)^{1/2} , \tag{4.9}$$

where

$$\cos\theta = H/(2H_E - H_A) . \tag{4.10}$$

For the experimental values of H, the value for $\cos\theta$ is always nearly zero. It can be shown that

$$A(\cos^2\theta - \sin^2\theta)^2 + (\cos^2\theta)/A \ll \sin^2\theta\,(A\cos^2\theta + 1/A) .$$

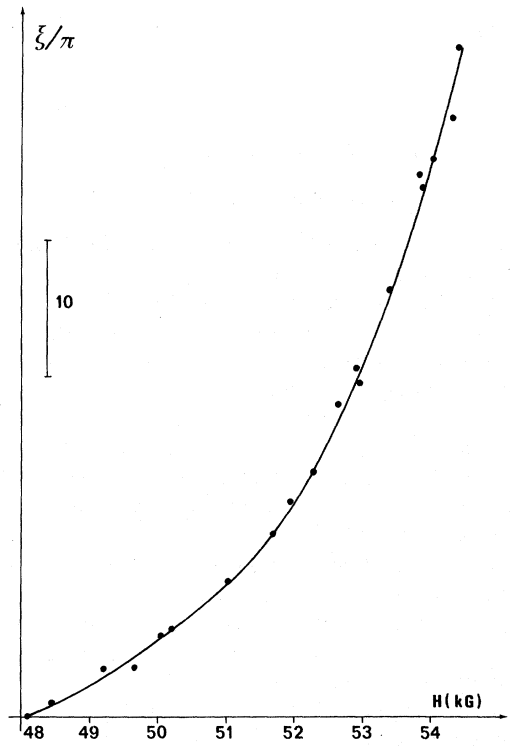

FIG. 6. Variations of ξ with magnetic field in the antiferromagnetic phase (arbitrary origin).

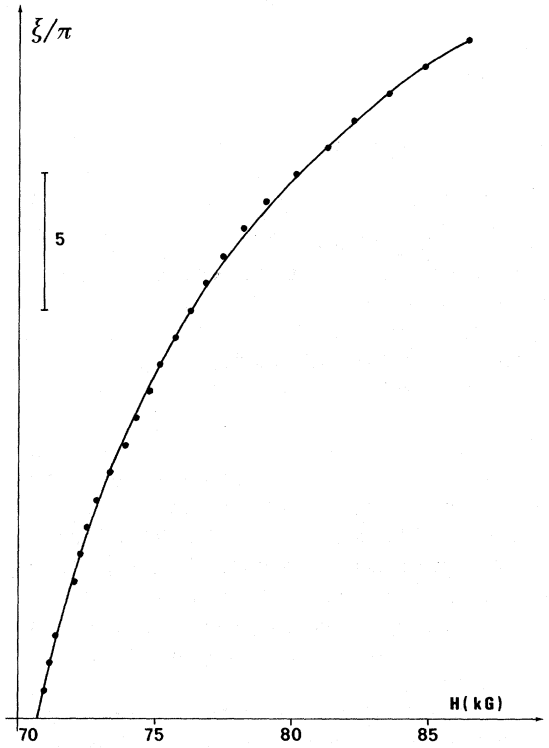

FIG. 7. Variations of ξ with magnetic field in the flopped phase (arbitrary origin).

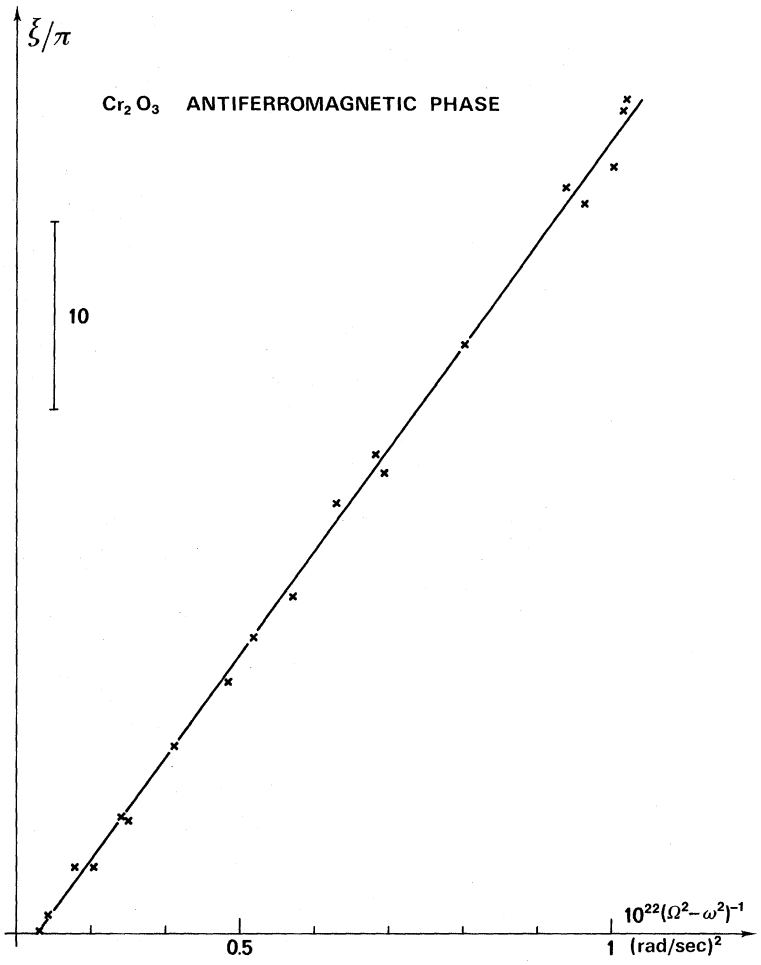

FIG. 8. Angle of rotation of the polarization as a function of $1/(\Omega_\beta^2-\omega^2)$ (antiferromagnetic phase).

Thus,

$$G^2 \simeq G_{46}^2 \sin^2\theta\,(A\cos^2\theta + 1/A)\ . \qquad (4.11)$$

Before comparing the developed theory with experiment, some comments, valid for both phases, will be made.

(i) Measurements of ξ/l versus $\vec{H}$ yield absolute values of the following coupling constants: $|G_{44}|$ in the antiferromagnetic phase and $|G_{46}|$ in the flopped phase.

(ii) There is a divergent factor $(\Omega^2-\omega^2)^{-1}$ in Eqs. (3.24) and (4.6). It may be thought that it introduces an infinite angle of rotation. But instead it must be kept in mind that these formulas are not valid if $\Omega \simeq \omega$ [condition (3.23a)]. On the other hand, phenomena such as attenuation, which becomes stronger near resonance, are neglected. This prevents, in any case, measurements near the crossing point.

(iii) Unlike the case of ferro- and ferrimagnetic compounds, there is no demagnetizing field. Therefore experimental results do not depend on the sample shape and are easily related with theory.

V. EXPERIMENTAL RESULTS

A. Experimental Technique

Ultrasonic waves are generated by the piezoelectric effect in an ac-cut quartz transducer introduced in a microwave cavity, the resonance frequency of which is about 9 GHz. The cavity is excited by a tunable magnetron. The ultrasonic pulses are detected by the inverse piezoelectric effect in the same quartz crystal after one round trip in the magnetic crystal (the Faraday effect on the two directions of propagation is cumulative, in contrast to the natural rotatory power where there is a cancellation). Such a transducer produces an elastic displacement parallel to the crystallographic x axis. Conversely, this cut is sensitive only to the x component of a transverse displacement and therefore behaves like an analyzer of transverse elastic waves.

A steady magnetic field up to 100 kG is produced by a superconducting coil. The orientation of the field along the easy axis of magnetization is adjusted by the following procedure: It is increased up to

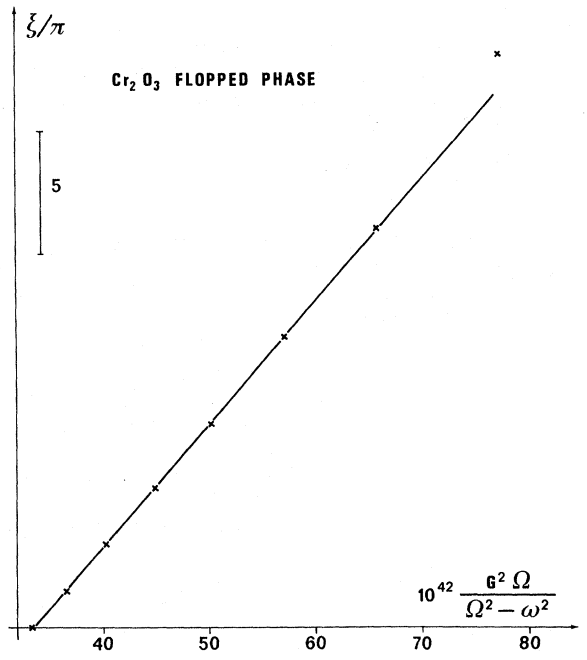

FIG. 9. Angle of rotation of the polarization as a function of $G^2\Omega/(\Omega^2-\omega^2)$ (flopped phase).

$H \simeq H_{sf}$ and the crystal is oriented such that the spin-flop transition occurs in the narrowest field range.

B. Results

The ultrasonic signal is detected and recorded with $\vec{H}$ varying from 0 to 85 kG. The internal conical refraction has no visible influence.

In Figs. 4 and 5, recordings of detected ultrasonic signals are reproduced for $H < H_{sf}$ and $H > H_{sf}$. The variations of ξ as a function of H are plotted in Figs. 6 and 7.

These figures show that the influence of the resonant phonon-magnon interaction is sensitive even rather far from the crossing point of the dispersion curves. In the antiferromagnetic phase, one of the excited magneto-elastic modes is strongly damped. In the flopped phase, the attenuation is large, and the oscillations of the ultrasonic signal are detectable only if the magnetic field is oriented accurately along the z axis.

C. Interpretation of Experimental Results

1. *Rotation in Antiferromagnetic Phase*

The ultrasonic waves interact with the low-frequency magnons obeying the dispersion law

$$\hbar\Omega_\beta(k) = g\mu_B H_E[(1 + H_A/H_E)^2 - \gamma_k^2]^{1/2} - g\mu_B H \ . \tag{5.1}$$

The dispersion curve is linear in k where $(ka)^2 > H_A/H_E$ and quadratic where $(ka)^2 < H_A/H_E$. It is easy to show that in Cr_2O_3, and with ultrasonic waves of 9 GHz, $(qa)^2 < H_A/H_E$ ($\vec{q}$ being the wave vector of noninteracting ultrasonic waves). Because of the uncertainty about the absolute measurement of the field, $\Omega_\beta(q)$ is not known with good accuracy; it is useful to introduce a fictitious magnetic field H_0 such that

$$\hbar\Omega_\beta(q) = \gamma(H_0 - H)$$

[see Eq. (3.10)].

The problem is then to determine the value of H_0 which gives a linear variation of ξ as a function of

$$\frac{1}{\Omega_\beta^2 - \omega^2} = \frac{1}{\gamma^2(H_0 - H)^2 - \omega^2} \ .$$

The best value is $H_0 = 60.5$ kG. This is to be compared to the experimentally determined spin-flop field, $H_{sf} = 58.5$ kG.

In Fig. 8 the variations of ξ as a function of $[\gamma^2(H_0 - H)^2 - \omega^2]^{-1}$ are plotted. The slope of this curve allows the determination of the magneto-elastic coupling constant G_{44},

$$|G_{44}| = 4.5 \text{ cm}^{-1} \text{ for } Cr^{3+} \text{ in } Cr_2O_3 \ .$$

2. *Rotation in Flopped Phase*

In the flopped phase, the dispersion law of the interacting spin waves considered here assumes the form

$$\hbar\Omega(k) = g\mu_B[H_E(1+\gamma_k)]^{1/2}[H_E(1+\gamma_k\cos 2\theta) - H_A\sin^2\theta]^2 \ .$$

The ultrasonic wave vector q is very small; it will be taken as

$$\hbar\Omega(q) \simeq \hbar\Omega(k=0) = g\mu_B(4H_E^2\cos^2\theta - 2H_E H_A\sin^2\theta)^{1/2} \ .$$

Then, by plotting the variations of the rotation as a function of $G^2\Omega/(\Omega^2-\omega^2)$ (Fig. 9) in the case of Cr_2O_3, the value of G_{46} is found,

$$|G_{46}| = 2.5 \text{ cm}^{-1} \text{ for } Cr^{3+} \text{ in } Cr_2O_3 \ .$$

The constants G_{ij} are defined in Eq. (2.5). From these numerical values, it can be easily deduced that the three conditions (3.23a)–(3.23c) are fulfilled.

VI. CONCLUSION

The experimental study of the acoustical Faraday effect in antiferromagnetic crystals at high frequency (9 GHz) shows that the interaction of phonon and spin waves originates in the coupling of each magnetic ion with the strain. This technique enables measurements to be made of some magneto-elastic coupling constants. Since in this frequency range the Faraday effect is quite large, these constants can be accurately determined. The numerical values found here may be compared to those measured by acoustical paramagnetic resonance on

diluted Cr^{3+} ions in corundum,[21] where Cr^{3+} substitutes for Al^{3+} without change of site symmetry,

$$G_{44}=1.85\ \text{cm}^{-1},\quad G_{46}=1.55\ \text{cm}^{-1}\ .$$

The present values are of the same order of magnitude.

The theoretical part of this paper can be transposed *mutatis mutandis* to other antiferromagnetic crystals of different symmetries provided the magnetization easy axis is an acoustical axis. This includes, for instance, the case of MnF_2.

†Work supported in part by the Délégation Générale à la Recherche Scientifique et Technique.

*Associated with the Centre National de la Recherche Scientifique.

[1]C. Kittel, Phys. Rev. 110, 836 (1958).

[2]H. Matthew and R. C. Le Craw, Phys. Rev. Letters 8, 397 (1962).

[3]R. Guermeur, J. Joffrin, A. Levelut, and J. Penné, Solid State Commun. 5, 369 (1967). The authors take this opportunity to point out that, when a parabolic law is supposed for the internal magnetic field along the rod, their result must be corrected to $b_2=12.9\times10^6\ \text{erg/cm}^3$ ($T=4.2$ °K, $\nu=10^{10}$ Hz). Value of H_A can be deduced: $H_A=-220$ G.

[4]R. Guermeur, J. Joffrin, A. Levelut, and J. Penné, Solid State Commun. 6, 519 (1968).

[5]J. R. Boyd and J. D. Gavenda, Phys. Rev. 152, 645 (1966).

[6]M. Boiteux, P. Doussineau, B. Ferry, J. Joffrin, and A. Levelut, Solid State Commun. 8, 1609 (1970).

[7]S. Foner, Phys. Rev. 130, 183 (1963).

[8]Y. Shapira, Phys. Rev. 187, 734 (1969).

[9]Y. L. Wang and H. B. Callen, J. Phys. Chem. Solids 25, 1459 (1964).

[10]S. V. Peletminskii, Zh. Eksperim. i Teor. Fiz. 37, 452 (1959) [Sov. Phys. JETP 37, 321 (1960)].

[11]M. A. Savchenco, Fiz. Tverd. Tela 6, 666 (1964) [Sov. Phys. Solid State 6, 864 (1964)].

[12]Y. Shapira and J. Zak, Phys. Rev. 170, 503 (1970).

[13]R. L. Melcher, J. Appl. Phys. 41, 1412 (1970).

[14]R. L. Melcher, Phys. Rev. Letters 25, 235 (1970).

[15]M. Boiteux, P. Doussineau, B. Ferry, and U. T. Höchli, J. Phys. Radium 32, 496 (1971).

[16]U. N. Upadhyaya and K. P. Shina, Phys. Rev. 130, 939 (1963).

[17]S. A. Al'tshuler, B. I. Kochelaev, and A. M. Leushin, Usp. Fiz. Nauk 75, 459 (1961) [Sov. Phys. Usp. 4, 880 (1962)].

[18]W. I. Dobrov, Phys. Rev. 134, A734 (1964).

[19]C. Kittel, *Quantum Theory of Solids* (Wiley, New York, 1963).

[20]E. J. Samuelsen, M. T. Hutchings, and G. Shirane, Physica 48, 13 (1970).

[21]P. L. Donoho, Phys. Rev. 133, 1080 (1964).

PHYSICAL REVIEW B VOLUME 4, NUMBER 9 1 NOVEMBER 1971

Scattering of Polarized Electrons from Magnetic Materials

L. Vriens

Philips Research Laboratories, N. V. Philips' Gloeilampenfabrieken, Eindhoven, The Netherlands

(Received 17 May 1971)

Cross-section formulas for large-angle (e, e) and for coincidence $(e, 2e)$ scattering of fast electrons from gaseous and solid targets are derived. It is shown that the momentum and spin-density distribution of the bound electrons can be obtained from single (e, e) scattering of polarized electrons. It is also shown that the electronic spin- and energy-dependent momentum-density distribution can be obtained from $(e, 2e)$ scattering of polarized electrons. An $(e, 2e)$ experiment with unpolarized electrons gives the energy-dependent momentum distribution. A comparison is made with related methods, like Compton scattering, and the feasibility of the suggested experiments is discussed.

I. INTRODUCTION

Recently, several papers[1-3,5-10] dealing with electron-momentum-density distributions in atoms, molecules, liquids, and solid materials have appeared. Three experimental techniques have been used for obtaining these distributions (a fourth less straightforward method is briefly discussed at the end of this paper).

The first method involves large-angle Compton scattering of x rays. Theoretical and experimental aspects of this method have been described in much detail by Eisenberger and Platzman,[1] Eisenberger,[2] and Currat *et al.*[3] The momentum distribution is obtained in this case from the frequency distribution of the x rays scattered through a fixed angle. The same information can be obtained from the angular distribution of x rays of a suitable frequency.

The second method involves large-angle and large-energy-loss scattering of fast electrons from gases or solids (reflection or transmission through thin films). This technique was applied already more than 30 years ago[4] for gaseous He and H_2. The momentum distribution is obtained either from the energy distribution[4] of the electrons scattered through a particular angle, or from the angular